


Received: November 15, 2022 Revised: March 24, 2023 Accepted: March 29, 2023

<https://doi.org/10.1016/j.neurom.2023.03.014>

Targeted Selection of Stimulation Parameters for Restoration of Motor and Autonomic Function in Individuals With Spinal Cord Injury

Claudia Angeli, PhD^{1,2,3} ; Enrico Rejc, PhD^{2,4};
Maxwell Boakye, MD, MPH, MBA^{2,4}; April Herrity, PhD, MBA^{2,4,5};
Samineh Mesbah, PhD²; Charles Hubscher, PhD^{2,6}; Gail Forrest, PhD^{7,8};
Susan Harkema, PhD^{2,3,4}

ABSTRACT

Study Design: This is a report of methods and tools for selection of task and individual configurations targeted for voluntary movement, standing, stepping, blood pressure stabilization, and facilitation of bladder storage and emptying using tonic-interleaved excitation of the lumbosacral spinal cord.

Objectives: This study aimed to present strategies used for selection of stimulation parameters for various motor and autonomic functions.

Conclusions: Tonic-interleaved functionally focused neuromodulation targets a myriad of consequences from spinal cord injury with surgical implantation of the epidural electrode at a single location. This approach indicates the sophistication of the human spinal cord circuitry and its important role in the regulation of motor and autonomic functions in humans.

Keywords: Epidural stimulation, neuromodulation, rehabilitation, spinal cord injury

Conflict of Interest: The authors report no conflict of interest.

INTRODUCTION

Emerging clinical data indicate that neuromodulation of the lumbosacral spinal cord restores motor and autonomic functions in those with chronic spinal cord injury (SCI).^{1–12} These discoveries provide evidence for the realistic potential of spinal cord epidural stimulation (scES) to significantly improve function in those with chronic, clinically incomplete and even complete SCI. However, 83% of the US physicians who participated in a dedicated survey¹³ perceive the lack of clear guidelines on

stimulation parameters as a significant barrier to the use of scES for functional improvement.

Two approaches to lumbosacral scES have shown motor and autonomic recovery for those with chronic SCI. One approach, described in this report, involves single placement of a 16-electrode array below the level of injury over the lumbosacral cord. An attached pulse generator positioned dorsally uses tonic-interleaved configurations that target optimization of the excitability state of the lumbosacral spinal cord, enabling the integration of appropriate sensory information and residual supraspinal influences to restore

Address correspondence to: Claudia Angeli, PhD, Department of Bioengineering, University of Louisville, 220 Abraham Flexner Way, Louisville, KY, USA 40202. Email: claudia.angeli@louisville.edu

¹ Department of Bioengineering, University of Louisville, Louisville, KY, USA;

² Kentucky Spinal Cord Injury Center, University of Louisville, Louisville, KY, USA;

³ Frazier Rehabilitation Institute, University of Louisville Health, Louisville, KY, USA;

⁴ Department of Neurological Surgery, University of Louisville, Louisville, KY, USA;

⁵ Department of Physiology, University of Louisville, Louisville, KY, USA;

⁶ Department of Anatomical Sciences and Neurobiology, University of Louisville, Louisville, KY, USA;

⁷ Human Performance and Engineering Research, Kessler Foundation, West Orange, NJ, USA; and

⁸ Department of Physical Medicine and Rehabilitation, Rutgers New Jersey Medical School, Newark, NJ, USA

For more information on author guidelines, an explanation of our peer review process, and conflict of interest informed consent policies, please see the journal's [Guide for Authors](#).

Source(s) of financial support: Claudia Angeli, Susan Harkema, Charles Hubscher, and Maxwell Boakye report financial support from the National Institutes of Health [1R01EB007615, 1UH3NS116238, 1OT2OD024898]. Susan Harkema reports financial support from the Leona M. & Harry B. Helmsley Charitable Trust [2011PG-MED011, 2016PG-MED001], the Craig H. Neilsen Foundation [ES2-CHN-2013], and the Christopher and Dana Reeve Foundation [ES_BI-2017]. Susan Harkema reports equipment, drugs, or supplies were provided by Medtronic Inc.

motor^{1–5,14–19} and autonomic function^{6–9} with integrated regulatory control. Another approach, typically referred to as epidural electrical stimulation, uses patterned spatial and temporal stimulation of the lumbosacral spinal cord specific for motor function^{10–12} and the thoracic spinal cord for blood pressure regulation.²⁰ Tonic-interleaved scES delivered at submotor threshold is designed to optimize the excitability of the spinal networks, enabling functional networks to emerge through integration of critical input. Patterned spatial-temporal scES delivers stimulation rhythmically to activate specific motor pools and can also be delivered through a closed-loop system acquiring timing related to the gait cycle from external sensors. The primary differences between the two approaches are presented in [Figure 1](#). Both strategies have been successful in restoring function in individuals with SCI.²¹

To date, the major challenges related to the selection of stimulation parameters for promoting motor and autonomic function recovery in patients with SCI are 1) these parameters are task- and individual-specific; and 2) the combination of stimulation parameters potentially available is vast, as exemplified by the >43 million different electrode configurations available when using a 16-electrode array. Several groups have published methods for scES configuration selection. Spatial mapping has been performed at low frequency (2 Hz), comparing vertical, horizontal, and diagonal configurations to define activation differences.²² This group suggests the use of spatial mapping as a starting point for the identification of more complex functional configurations. Once a spatial configuration is selected, by the preference of the participant, temporal optimization is performed by probing multiple frequency and pulse-width alternatives.²³ A Bayesian model used to analyze at-home temporal selections is then applied to predict the patient-specific preference model to explore a broader set of temporal parameters. This model was applied to configurations that targeted voluntary movement as the primary outcomes. Hofstoetter et al²⁴ developed a statistical model to predict cathode-location selectivity for the activation of motor pools. Those authors used motor evoked responses from low-frequency scES to map the motoneuron pools for the rectus femoris and hamstring muscles and further expansion to a detailed anatomical organization of the motor pools across the lumbosacral spinal cord. They also confirmed the correlation between intraoperative and post-operative mapping. Mapping for spatiotemporal scES starts with the optimization of electrode position during surgical implantation.^{12,25} The team uses a personalized model of the spinal cord to accurately predict muscle responses and develop a personalized model. Optimization of stepping configurations is performed by attempting selective configurations based on the personalized model, and fine-tuning anode-cathode combinations based on the observed movements.^{12,25} Once configurations are optimized, the timing and sequence of stimulation are selected for each participant. There is consensus that a key aspect of developing functional stimulation configurations is the understanding of specificity of stimulation location relative to motor activity for each individual.^{12,22,24,25} However, the strategies used to reach functional motor configuration vary across research groups. Three components guide tonic-interleaved functionally focused scES. First, a neuroanatomical three-dimensional (3D) spinal cord reconstruction model and intraoperative evoked potentials inform electrode lead placement. Second, spatial-temporal electrophysiological mapping informs motor and autonomic mapping. Last, task-specific motor mapping (leg movements, standing, and stepping) and autonomic mapping (blood pressure regulation, bladder capacity, and

initiation of bladder void) identify the tonic-interleaved functionally focused scES parameters. Immediate integrated movement and physiological responses to scES indicate the sophistication of the human lumbosacral spinal circuitry, with a critical role in ongoing regulation of motor and autonomic function. The aim of this study is to present strategies for the selection of functional tonic-interleaved scES configuration.

MATERIALS AND METHODS

We developed the methods presented later from data collected across multiple projects with various scES intervention paradigms ranging from motor (standing, stepping, and voluntary movement) to autonomic function (cardiovascular [CV] regulation and bladder capacity and emptying). A total of 47 research participants underwent implantation across all projects, with an average age of 34.4 ± 10.2 years (range: 19.9–60.5 years), at an average of 9.0 ± 7.8 years after injury (range: 0.5–38.6 years). Of the 47 participants, 16 were women. Twenty-nine participants were classified as AIS-A, 15 as AIS-B, and three as AIS-C. Eight of 47 had sustained a thoracic injury (T1–T5), with the rest having cervical injuries (C3–C8). The research participants signed an informed consent for electrode implantation, stimulation, interventions, and physiological monitoring studies approved by the University of Louisville Institutional Review Board.

The initial 13 participants underwent implantation with a voltage-controlled RestoreADVANCED (Medtronic, Minneapolis, MN) neurostimulator. All remaining participants underwent implantation with a current-controlled Intellis™ (Medtronic) neurostimulator. All 47 participants underwent implantation with a 5-6-5 Specify (Medtronic) electrode array. Of 47 participants, 46 (98%) have been mapped for voluntary movement and standing; 13 of 47 have been mapped for stepping; 36 of 47 have been mapped for CV function, and 11 of 47 have been mapped for bladder function. Equipment and personnel for each function will vary and are included in the [Supplementary Data](#).

Neuroanatomical 3D Spinal Cord Reconstruction Model and Surgical Implantation

Before surgery, participants undergo a magnetic resonance imaging (MRI) scan that includes obtaining sequential axial T₂-Turbo Spin echo images from the T10–S1 vertebrae with high spatial resolution (3 mm axial thickness and zero gap) using a Siemens 3.0 Tesla MAGNETOM Skyra with Turbo Spin Echo (Siemens Medical Solutions, Malvern, PA). A 1.5 Tesla (General Electric, Milwaukee, WI) is appropriate in cases in which hardware implants contraindicate higher magnet strengths. We observed considerable variability among individuals regarding the location of conus termination with respect to vertebrae, ranging from vertebrae T12 to L2.²⁶ The length of the lumbosacral spinal cord also varies across individuals, and therefore, the location of spinal cord levels L1–S1 also varies with respect to the vertebral bodies.²⁶ The neuroanatomical 3D spinal cord reconstruction from sequential axial images that includes dorsal root tracing provides a more precise determination of the neuroanatomical characteristics of the spinal cord. The 3D spinal cord reconstruction methods have been described in more detail in a previous publication.²⁷ During surgery, the objective is to place the electrode paddle midline of the vertebral column over the L1–S1 spinal cord levels while covering a significant area of the lumbosacral enlargement.^{28,29}

Region-of-interest tracing (Mango software, Research Imaging Institute, UTHSCSA) of the circumference of the spinal cord, the dura border, and dorsal roots generates a 3D visual model of the spinal cord. Nerve root tracing from the sequential axial images of the locations where the nerve roots exit the vertebrae and emerge into the spinal cord results in the identification of the L1–S1 spinal cord levels at the lumbosacral enlargement. These levels are then delineated on the 3D visual model. The neuroanatomical 3D reconstruction model was generated (Fig. 2a–c) from quantitatively integrating the sagittal images of the vertebrae, the known dimensions of the scES paddle (Medtronic Specify® 5-6-5 lead, 46.5

mm), and the location of the nerve roots emerging from the spinal cord.

Before the implant, possible positions of the electrode paddle are projected onto the MRI-based 3D model, and corresponding percentages of lumbosacral enlargement coverage are calculated. This information is used in the identification of the level of surgical laminotomy. In most individuals, the length of the lumbosacral enlargement is greater than the total length of the electrode contacts in the scES paddle, and therefore, the placement is informed by the knowledge of those lumbosacral spinal cord levels that have been most successful in the recovery of deficits.

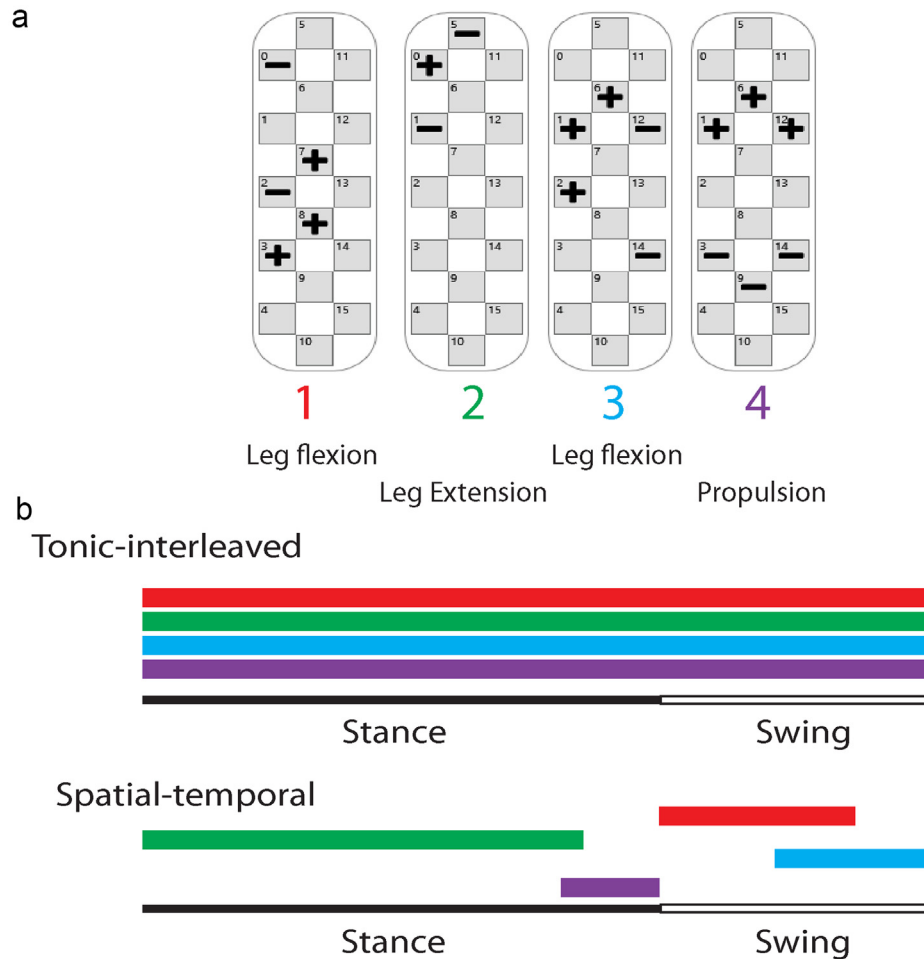


Figure 1. Comparison between scES types. a. Example of stimulation configuration using multiple programs to target different functions. b. Sample timing of programs for tonic-interleaved and spatiotemporal stimulation types. c. Table of characteristics of stimulation by type.

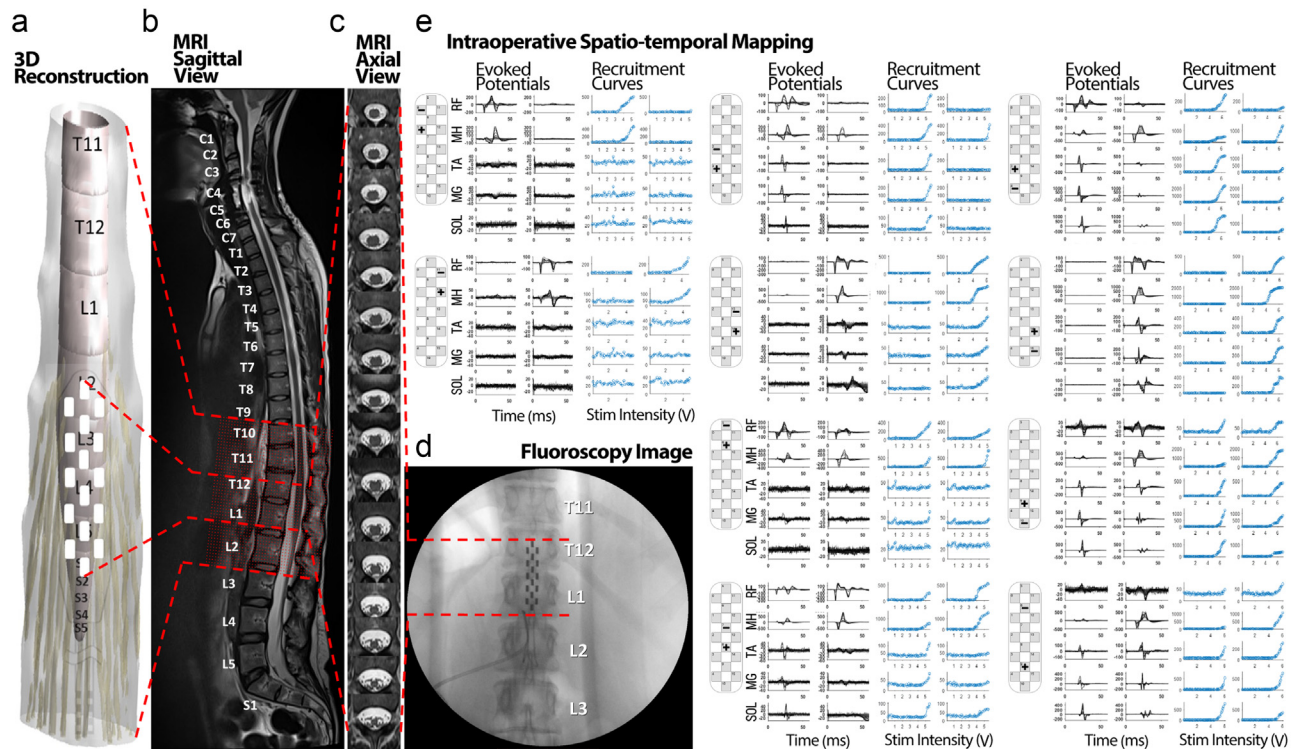


Figure 2. Surgical paddle placement procedure. a. Preoperative MRI-based neuroanatomical 3D reconstruction of spinal cord with scES paddle placement. b. Spinal cord MRI in sagittal view. c. High-resolution axial MRI scans. d. Intraoperative fluoroscopy image with red dashed lines showing integration of x-ray and MRI scans to estimate the paddle placement with respect to the spinal cord levels. e. Intraoperative spatiotemporal mapping shown with overlaid evoked potentials (black) and recruitment curves (blue) of muscle responses to the stimulation with various electrode combinations including unilateral (left and right columns) and middle column two-electrode combinations at rostral, caudal, and middle part of the scES paddle array. Electromyography is recorded from RF, MH, TA, MG, and SOL. MG, medial gastrocnemius; TA, tibialis anterior.

After the initial positioning of the electrode array, intraoperative evoked potentials are elicited, and muscle activation thresholds and amplitude response curves are evaluated in real time (Fig. 3a). Midline and rostral-caudal positioning of the paddle is refined to optimize the motor evoked responses of key muscles (Fig. 3b). Fluoroscopy images of the selected placement are recorded and used by the analytical team to recalculate the spinal cord coverage.

Spatiotemporal Mapping

Spatiotemporal electrophysiological mapping is the first step in identifying the spatial relationship between stimulation site and motor evoked responses in specific muscles. During this process, we identify the threshold and temporal relationships of lower extremity muscles. Spatiotemporal mapping typically occurs two to three weeks after implant, over two to three days, and is performed while the individual rests supinely. During these sessions, electromyography (EMG) of eight lower extremity muscles (soleus [SOL], medial gastrocnemius, tibialis anterior, medial hamstrings [MH], vastus lateralis [VL], rectus femoris [RF], gluteus maximus, and iliopsoas) is bilaterally recorded. After standard skin preparation, surface electrodes with fixed interelectrode distance are placed parallel to the muscle fibers over the muscle belly. Ground electrodes are placed bilaterally over the distal tibia. A disposable fine-wire electrode (44 ga) is inserted through a 27 mm needle to record activity from the iliopsoas. Bony landmarks are used to guide the localization of the needle insertion point.³⁰ The onset of each stimulation pulse is identified through the scES artifacts recorded by two surface electrodes placed symmetrically over the paraspinal

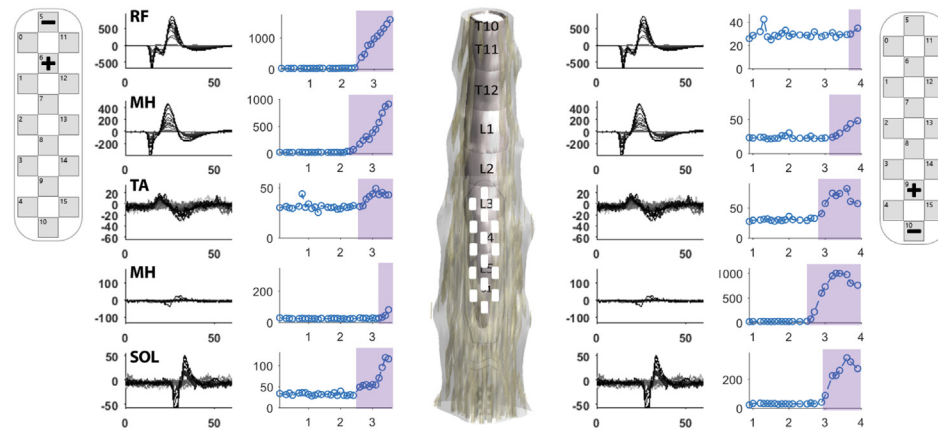
muscle, adjacent to the electrode array incision. Continuous beat-to-beat blood pressure is also monitored throughout the mapping session (Finapres Medical Systems, Amsterdam, The Netherlands). A 32-channel hard-wired AD board and custom-written acquisition software (LabView, National Instruments) record all signals at 2000 Hz. EMG signals are filtered using a band-pass filter of 10 to 2000 Hz (−3 dB). scES artifact is only present on the paraspinal muscle signal; this artifact is used to determine the exact timing of each stimulation pulse during low-frequency mapping.

Spatiotemporal mapping is performed using a pulse width of 1000 μ sec and consists of four sections: 1) bipolar midline amplitude response; 2) bipolar lateral amplitude response; 3) wide-field amplitude response; and 4) wide-field frequency response. The maximum allowable pulse width for the IntellisTM neurostimulator is 1000 μ sec pulse width and is selected owing to the stronger responses expected at longer pulse width durations.

1. Bipolar midline amplitude response

Ten bipolar combinations are tested along the middle column during the initial amplitude response with a stimulation frequency of 2 Hz (Fig. 4a). Adjacent anode and cathode electrodes are selected in the middle column, and combinations are randomized for each participant. The adjacent electrodes provide the smallest electrical field among electrodes and are selected for testing to increase the specificity and selectivity of responses. We perform all possible combinations in the middle column of the array to

a Spatio-temporal Mapping for Surgical Paddle Placement at L3-S Spinal Cord



b Spatio-temporal Mapping for Surgical Paddle Placement at L2-L5 Spinal Cord

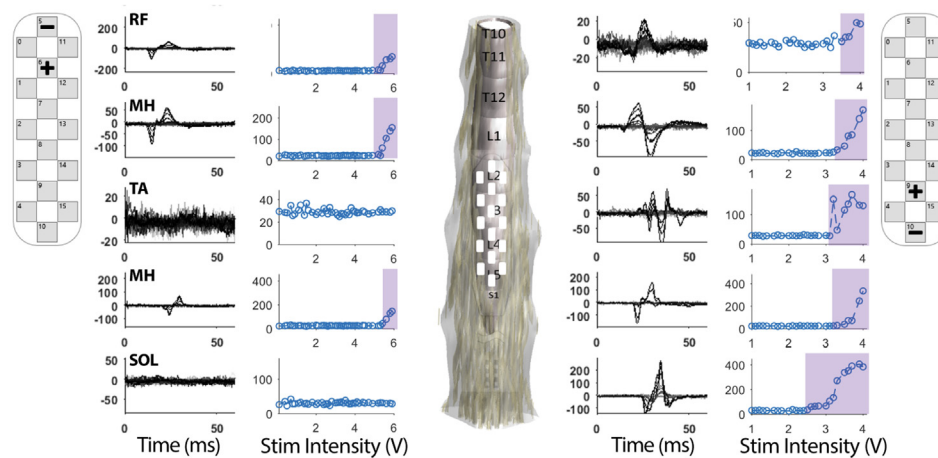


Figure 3. Intraoperative spatiotemporal mapping. Overlaid evoked potentials (black) and recruitment curves (blue) for two scES paddle placements on the spinal cord during placement adjustment. a. scES paddle electrode is placed at L3–S lumbosacral spinal cord, and b. paddle electrode is moved to L2–L5. Electromyography is recorded from RF, MH, TA, MG, and SOL. MG, medial gastrocnemius; TA, tibialis anterior.

maximize the bilateral activation of the lower extremity muscles and to identify physiological differences between left and right sides throughout the length of the electrode array. Stimulation starts at 0.1 mA or the highest prethreshold amplitude, and is increased by 0.1 mA until all assessed muscles have reached motor threshold. For this purpose, motor threshold is defined as the lowest stimulation amplitude that elicits a motor evoked potential with minimum amplitude and appropriate latency to the stimulation artifact. The activation detection method to identify the motor threshold has been described previously.³¹ In short, the denoised signal is modeled by a Gaussian probability density function for which parameters are estimated using a maximum likelihood estimation method. The Gaussian model of all the EMG responses is then compared with the Gaussian model of the background noise, and the highest statistical difference between the response and the background noise is calculated. We then calculate a dynamic threshold to find the first segment of the signal that includes an evoked response.³¹ Once all muscles are active, the amplitude response test continues at increments of 0.5 mA until all muscles have reached a plateau in the peak-to-peak amplitude, maximum stimulation is reached, the blood pressure response has increased

>160 mm Hg systolic, as recommended by the study cardiologist, or the participant requests to stop.

2. Bipolar lateral amplitude response

The bipolar lateral amplitude response follows the same process as the midline amplitude response, except three combinations are chosen for each side to represent a rostral, middle, and caudal location (Fig. 4b). Selecting bipolar configurations on the left and right columns of the electrode array provides the research team with parameters that target single limb activation. As shown in Figure 4b, a true unilateral activation is not typical; therefore, understanding the differences in amplitude and threshold is critical to identify side-specific functional configurations. Time efficiency was the deciding factor to restrict the lateral configurations to three per side. Previous data on three participants mapped using all possible anode/cathode combinations on the lateral columns did not support the need for the additional specificity. In contrast to bipolar configurations, wide-field configurations provide generalized activation patterns that can be useful to understand responses to frequency variations.

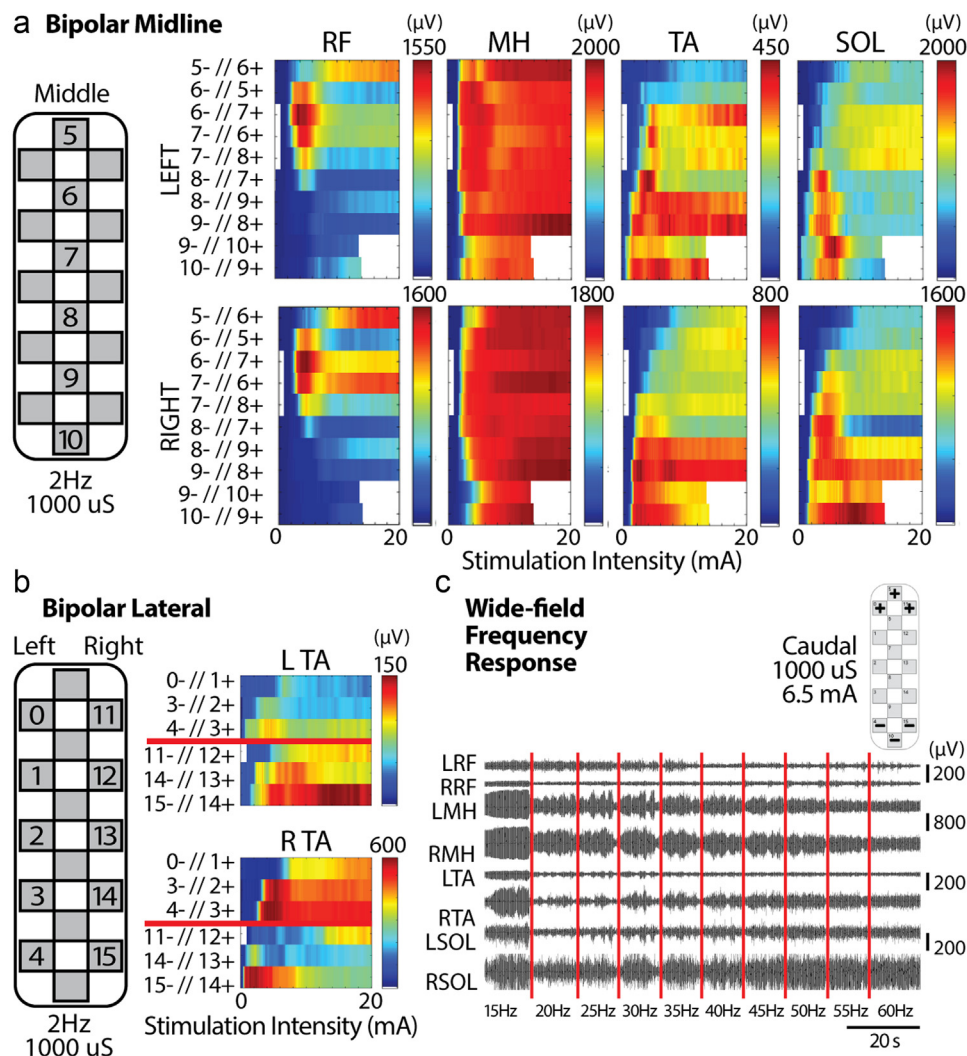


Figure 4. Spatiotemporal mapping. a. Color maps depicting the peak-to-peak amplitude values (μV) corresponding to stimulation current (mA) and electrode configuration (numbers in each row refer to contacts of the electrode array tested shown to the left). All combinations are in the middle column of the electrode array. Selected left (top) and right (bottom) muscles: RF, MH, TA, and SOL are shown. b. Color maps depicting the peak-to-peak amplitude values (μV) corresponding to stimulation current (mA) and electrode configuration (numbers in each row refer to contacts of the electrode array tested shown to the left). All combinations are in the lateral columns of the electrode array. Left tibialis anterior (LTA) (top) and right tibialis anterior (RTA) (bottom) are shown. c. EMG responses for left and right muscles for a caudal wide-field frequency response. Red lines identify the time of frequency increase whereas the amplitude remains constant at 6.5 mA. RTA, right tibialis anterior; TA, tibialis anterior.

3. Wide-field amplitude response

The wide-field amplitude response is performed with the top three electrodes (0, 5, 11) and bottom three electrodes (4, 10, 15) selected as cathodes and anodes. Both rostral and caudal configurations are tested. Wide-field configurations are used to generate a stronger field that spreads across the full length of the lumbosacral spinal cord covered by the electrode array. This stronger field will generate activation across all muscles at lower stimulation amplitudes, leading to a narrower amplitude range for motor thresholds across all muscles. For the wide-field configurations, stimulation amplitude starts at 0.3 mA and continues in increments of 0.3 mA; stopping can occur for the same reasons as previously mentioned. Although a wide-field configuration is not typical for functional outcomes, it provides a basis for the selection of

stimulating amplitudes during the frequency response curves. Reaching maximum peak-to-peak responses across all muscles tested is common while stimulating with a wide-field configuration.

A comparison of certain components of the above detailed mapping is also performed with a pulse width of 450 μsec . This included selected midline rostral, middle, and caudal bipolar configurations and the rostral and caudal wide-field configurations. The rationale to compare these selected configurations was the initial limitation of 450 μsec as the highest pulse width in the RestoreADVANCED neurostimulator. Although it provides an internal comparison across our data sets, collection at two different pulse widths is recommended to understand the amplitude-to-pulse-width relationship in each research participant. A pulse width of 1000 μsec will limit the frequency range available for programming; therefore, functional configurations will have to balance optimal frequency with optimal pulse width and stimulation intensity.

4. Wide-field frequency response

Frequency responses are performed to understand at which frequency independent muscles are most likely to reveal tonic, bursting, or step-like patterns. A frequency response is performed with the wide-field configurations at two different stimulation amplitudes. The first stimulation amplitude, considered low, is selected after the onset of all muscles as determined in the 2 Hz wide-field amplitude response. The muscle with the latest (highest stimulation amplitude) motor threshold is used in this selection. The amplitude selected will be near the lower third of the recruitment curve slope. A second stimulation amplitude, considered high, represents a range on the top one-third of the slope, close to the peak-to-peak plateau. We test frequencies from 15 Hz through 100 Hz in increments of 5 Hz; each frequency is assessed for 10 seconds (Fig. 4c). Elevation in blood pressure and discomfort are typical reasons that 100 Hz is not reached and can be most common in the high amplitudes. The high amplitude response is repeated with a 450 μ sec pulse width. Although both amplitudes can be repeated at the lower pulse width, in most cases, the low amplitude will be too low for activation of all muscles and results in no muscle activation at the higher frequencies. This evidence was obtained by repeating both amplitude intensities at 450 μ sec in 13 participants. The frequency response data are valuable in identifying activation patterns (locomotor, bursting, and tonic) through the various frequencies. Importantly, frequency response data provide valuable information to identify frequency ranges in which muscle activity starts to decrease. Muscle activity inhibition can strategically be used to combine stimulation programs targeting the increased activity in some groups and inhibition in others to optimize the functional outcome.

To gather more information with direct translation to functional configuration, a 30 Hz amplitude response is performed at selected rostral, middle, and caudal bipolar configurations in addition to wide-field configurations. Typical frequencies for rhythmic motor activation range from 25 Hz to 50 Hz.³² A frequency of 30 Hz allowed standardization across participants. This additional amplitude response is performed at both 1000 μ sec and 450 μ sec pulse widths. Identification of bursting patterns by location, amplitude, and pulse width will provide key information for functional mapping of voluntary movement, standing, and stepping.

All 2 Hz data are analyzed and visualized using previously described methods.³¹ Briefly, a custom five-step algorithm framework was written in Matlab (MathWorks, Natick, MA) to detect motor evoked potentials activation through the stimulation range, extract key features such as peak-to-peak amplitude, latency, and integrated EMG values, and visualize results using color map images for ease of interpretation.³¹ Color maps are generated to easily visualize the amplitude of each motor evoked response relative to stimulation intensity for each muscle and electrode selection (Fig. 4).

Selection of scES Electrode Configuration for Voluntary Movement

Voluntary movement requires a configuration that increases the excitability of a specific area of the spinal cord but remains at submotor threshold.¹⁵ A submotor threshold configuration optimized for a specific voluntary action allows the integration of supraspinal signals by the spinal networks, resulting in the intended movement. Evaluation of the heat maps generated from the spatiotemporal mapping will provide a starting point for distribution of cathodes and anodes. Heat maps need to be evaluated to 1) identify stimulation amplitude

for onset of motor activity relative to cathode and anode location; 2) identify peak-to-peak changes relative to stimulation amplitude and identify stimulation amplitude at which maximum peak-to-peak amplitude is achieved; 3) identify the relationship for onset of motor activity and maximum peak-to-peak amplitude between antagonistic muscles; and 4) identify left-to-right differences on the same muscle. An important aspect to consider is the activation of the tibialis anterior. The tibialis anterior is activated during the execution of ankle dorsiflexion and during hip flexion from a supine position owing to the kinetic chain engaging the ankle during full range of motion. Figure 4a provides a decision-making flowchart to guide investigators mapping for voluntary movement. In addition to the 2 Hz spatiotemporal mapping analysis, the frequency response data and 30 Hz spatiotemporal mapping data are used to understand coactivation and alternation patterns of specific muscle groups and the frequencies that promote bursting and alternation patterns, or an overall reduction in muscle activity (Fig. 5b,c). In the example provided in Figure 4c, a configuration at the most rostral aspect of the electrode array does not produce bursting while maintaining the same stimulation intensity, and moving down one segment produces bursting of the iliopsoas and tibialis anterior. Although a caudal configuration also produces bursting, it results in coactivation of flexors and extensors. The specificity of these results suggests an initial location of cathodes toward the middle of the electrode array as a starting point for assessing voluntary activity.

Assessment of configurations for voluntary leg movement initially takes place in a supine or a semireclined position (15°–30°). The initial configurations are tested by slowly increasing stimulation amplitude and asking the individual to perform the intended action. Stimulation amplitude should be increased until the individual can perform the movement. If the stimulation leads to the activation of the agonist, a supramotor threshold state has been achieved, and parameters must be revisited. Stimulation amplitude must remain at submotor threshold for the agonist and synergistic muscle groups. A submotor threshold stimulation state promotes integration of residual input and sensory information, as opposed to inducing the movement.

Multiple attempts might be required for the individual to decipher how to interact with submotor threshold stimulation. In most cases, individuals have been injured for more than two years without attempting to perform voluntary movement of their paralyzed lower extremities. It is imperative for the investigator leading the assessment to guide the individuals on the basis of electrophysiological data and suggest strategies for accessing the appropriate networks. A change in stimulation amplitude inducing a small joint movement or a single EMG burst on the agonist muscle indicates that the location of anode and cathode distribution is appropriate. In those cases, the stimulation amplitude and frequency remain to be adjusted (Fig. 5d). Early in the mapping phase, small changes to electrode selection might greatly affect the ability of the individual to perform the desired movement. Because the individual learns to integrate the stimulation with the supraspinal intent, stimulation parameter changes do not affect the performance of the task as dramatically as during the early phases.

Selection of scES Electrode Configuration for Standing

Dedicated guidelines were developed to determine the subset of electrode configurations to be tested for facilitating standing. These guidelines were based on the available literature and on spatiotemporal mapping assessments performed in a supine

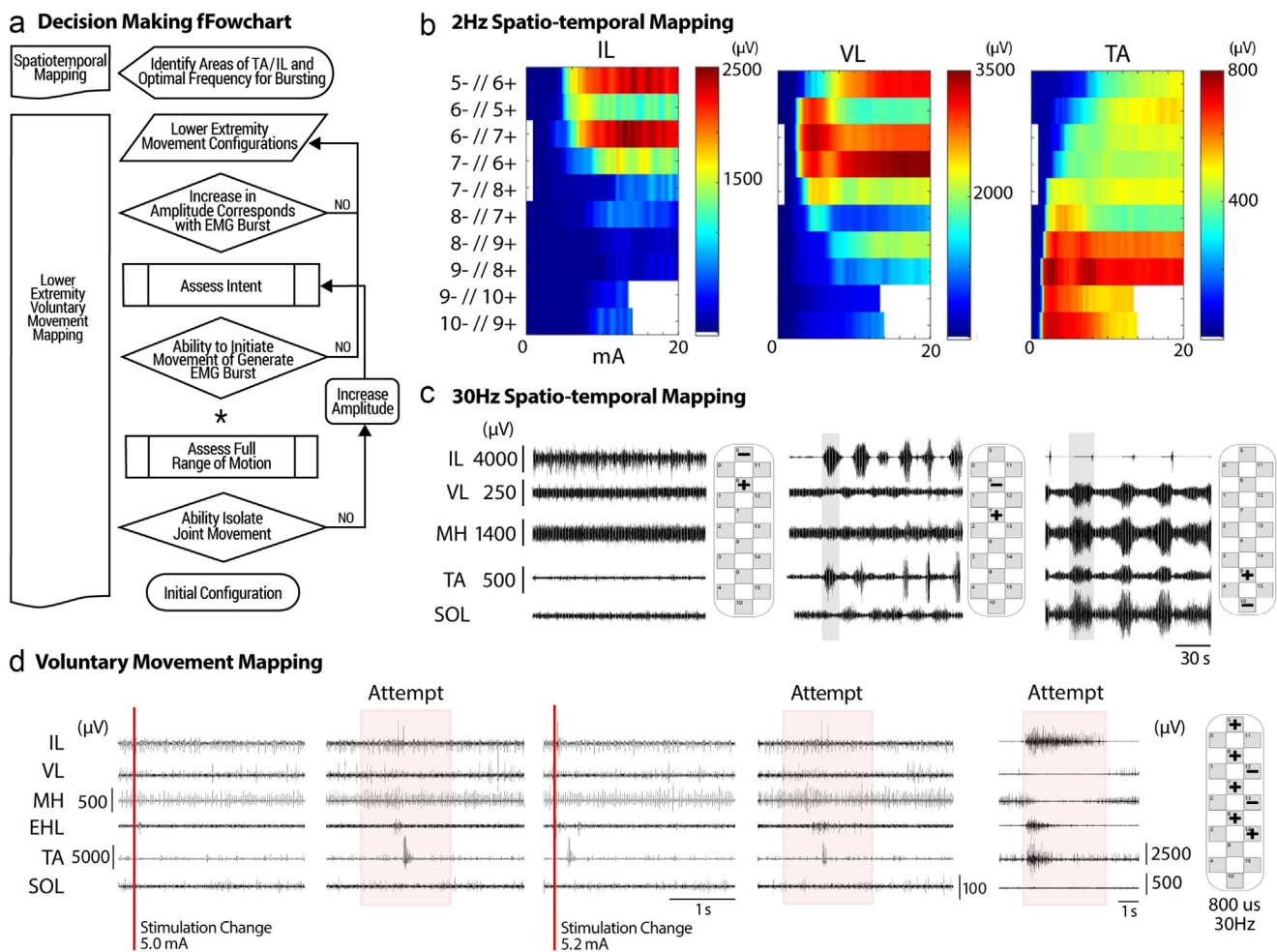


Figure 5. Selection of scES parameters for voluntary movement. a. Decision-making chart for the selection of configurations. Spatiotemporal mapping is used to identify the areas of the electrode array where TA and IL activity is present. An initial configuration is represented as the data (parallelogram); decisions in the process are represented by rhomboids. If the response to the question is YES, one continues down the flowchart; if NO, the flowchart will guide one to the restarting point. A predefined process (rectangles) will expand on the assessments needed to optimize the configuration, and it is typically followed by a decision. An alternate process (rounded-corner rectangles) can be inserted late in the flowchart if a complex decision is not achieved, promoting a small modification to the configuration and restarting linking back to a predetermined process. The asterisk (*) signifies a stopping point if full range of motion cannot be achieved during the mapping process. b. Color maps depicting the peak-to-peak amplitude values (μV) corresponding to stimulation current and electrode configuration (numbers in each row refer to contacts of the electrode array tested for the IL, VL, and TA muscles). c. EMG activity of representative leg muscles during 30 Hz spatiotemporal mapping at three different electrode locations. Epidural stimulation programs applied are reported to the right side of each panel. Amplitude ranges are the same in all three locations, producing different activation patterns. d. EMG activity of representative leg muscles during amplitude increases and voluntary attempts in a mapping session. Bottom panel represents the optimal configuration at 6.5 mA, generating appropriate range of motion. Epidural stimulation program is reported at the bottom panel, and it is the same for all attempts. EHL, extensor hallucis longus; IL, iliopsoas; TA, tibialis anterior.

position. Electrode fields more focused on the caudal portion of the electrode array (ie, spinal cord segments L5–S1) can be selected to promote activation of distal muscle motoneuron pools, whereas electrode fields focused on the rostral portion of the array (ie, spinal cord segments L1–L2) can be activated to promote activation of the proximal muscle motoneuron pools.³³ In addition, in case of activation differences between left and right lower limb, active electrodes can be unbalanced between lateral columns of the electrode array because the lateral placement of the epidural stimulation electrodes with respect to the spinal cord midline was shown to promote motor responses in muscles ipsilateral to the stimulation.³⁴ We successfully facilitated standing through applying high stimulation frequencies (ie, 25–60 Hz) at near-motor threshold stimulation amplitudes that did not directly elicit lower limb movements in sitting.¹⁸ In particular, the application of higher

stimulation frequencies can favor the integration of afferent input and residual supraspinal input through the greater involvement of interneurons,^{32,35} and results in a more physiological (ie, non-pulsatile) muscle contraction. Hence, scES for standing is initially delivered at a near-motor threshold stimulation amplitude that does not directly elicit lower limb movements in sitting. Stimulation amplitude and frequency are then synergistically modulated during standing to identify the higher stimulation frequency that can elicit a continuous (nonrhythmic) EMG pattern effective in bearing body weight.

The decision-making process of the selection of scES parameters to facilitate standing is depicted in Figure 6a, and exemplary outcomes for a representative research participant with motor complete SCI and cervical level of injury (B38) are reported in Figure 6c–g. Individualized activation maps (Fig. 6b) suggested

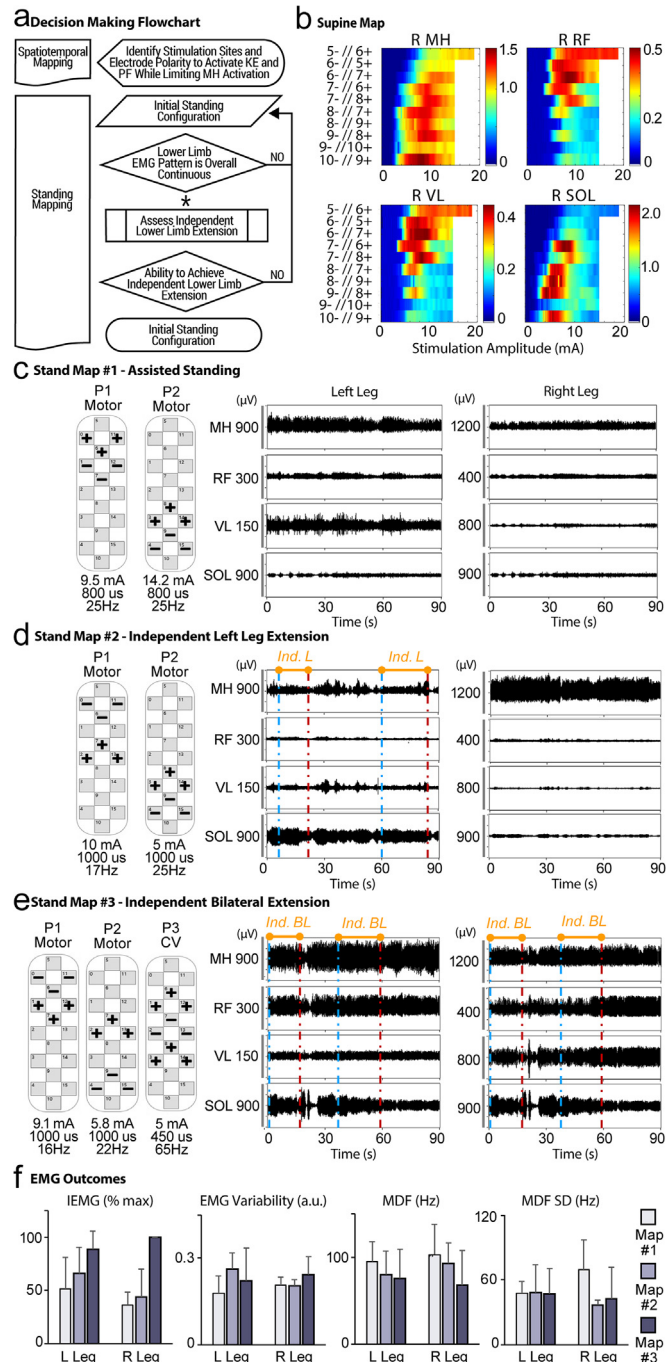


Figure 6. Selection of scES parameters for standing. **a.** Decision-making flowchart for the selection of stimulation parameters for standing. Spatiotemporal mapping assessed in supine position is used to identify the electrode array contacts and the related polarity eliciting the activation of KE and PF while limiting the activation of MH. After the initial stimulation configuration (parallelogram) is defined, decisions in the process are represented by rhomboids. If the response to the question is YES, the flow continues vertically down; if NO, the flowchart will guide one to the restarting point. A predefined process (rectangle) will expand on the assessment needed to optimize the configuration, and it is followed by a decision. If the decision outcome is negative, an alternative process (rounded-corner rectangle) is included to allow small adjustments of the stimulation parameters and restarting back to a predetermined process. In case the mapping process does not result in the targeted functional outcome (achieve independent lower limb extension), stimulation configuration may be determined at the flowchart level identified with the asterisk (*). **b.** Color maps depicting the peak-to-peak amplitude values (μV) corresponding to stimulation current and electrode configuration (numbers in each row refer to contacts of the electrode array reported in panel a) tested for the R, MH, RF, VL, and SOL muscles). **c–e.** EMG activity of representative right and left leg muscles during different stand mapping sessions (#1 to #3, respectively). Ind. of the L leg, or of BL concurrently, is indicated by the time windows within vertical dotted lines. Epidural stimulation P applied are reported to the right side of each panel. In panel e, P3 was added to target the increase in blood pressure because the persistent low blood pressure experienced by the participant limited standing bout duration. **f.** EMG variables (IEMG, MDF, MDF SD) associated with standing ability in this population, which were calculated over the 90-second data sets shown in panels c, d, and e. BL, both legs; IEMG, integrated EMG; Ind., independent extension; KE, knee extensors; L, left; P, programs; PF, plantar flexors; R, right.

focusing stimulation on the spinal cord segment L3, corresponding to the rostral part of the array (6- / 7+) to engage knee extensors (RF and VL) while limiting the activation of knee flexors (MH). Electrode configuration of P1 (Fig. 6c–e) was selected to facilitate this motor outcome. Cathodes were initially placed more caudally than were anodes (as supported by literature^{32,36,37}; Fig. 6c), and then reversed (Fig. 6d–e), as suggested by the higher activation promoted for VL and RF in supine position by the anode placed more caudally than the cathode (“6- / 7+” vs “7- / 6+,” Fig. 6b). Electrode field of P2 (Fig. 6c–e) initially targeted the spinal cord segments L4–L5 to facilitate the activation of plantar flexor muscles as suggested by the individualized activation maps (Fig. 6b, SOL, electrodes “9- / 8+”), and was subsequently extended (Fig. 6e), covering L3–L5 spinal segments, to further contribute to the activation of more proximal motor pools. Stimulation frequency of P1 and P2 was slightly decreased, and pulse width increased, throughout the standing map process (Fig. 6c–e) to facilitate extension pattern and higher muscle activation. Along with the process of standing stimulation mapping, a stimulation program targeting the increase in blood pressure (P3, Fig. 6e) was added because of the persistent low blood pressure that limited standing duration. The described adjustments in stimulation parameters progressively improved functional outcomes represented by the transition from no independent lower limb extension, to bouts of independent extension of the left lower limb, to bouts of bilateral lower limb extension (Fig. 6c–e). This was associated with changes in activation pattern characteristics (Fig. 6f) resulting in trends of higher EMG amplitude, lower median frequency (MDF), and lower MDF SD (for the right lower limb). As previously described by our group while assessing >400 standing bouts generated by 11 research participants,³⁸ these trends are consistent with an improved effectiveness of EMG pattern for standing with scES. MDF and MDF SD are EMG-frequency domain features calculated by Continuous Wavelet Transform using Morlet wavelet.³⁸ Instantaneous MDF values are initially calculated, and their average and SD for the time windows of interest are considered for analysis. Generally, standing bouts with fixed scES parameters lasting at least 40 seconds were identified, and the initial and final 5 seconds of each bout were discarded from analysis. The number of stimulation parameters tested during each standing mapping session could vary for each individual depending on their physiological responses to scES, including their ability to maintain an upright position because of blood pressure regulation, and their subjective feedback, including the level of comfort in exploring novel sets of stimulation parameters. Seated resting periods could be requested by the participants at any time and were also administered by the investigator with the goal of testing stimulation parameters without evident signs of fatigue (ie, considering breathing and talking pattern).

Selection of scES Electrode Configuration for Facilitating Stepping

The selection of anode and cathode distribution, number of cohorts, and stimulation frequencies is based on the spatiotemporal mapping data; in addition, the standing and voluntary configurations provide key information used in optimization (Fig. 7a–c). The voluntary movement configuration informs the team on the location and distribution of electrodes for hip flexion and ankle dorsiflexion, key aspects of the swing phase. The standing configuration informs the team on areas that promote knee extension in addition to the required frequencies.

Although stepping is not a simple combination of functional tasks such as knee extension and hip flexion, the previous configurations allow an initial starting point for the selection of cohorts. A cohort is defined as a group of active electrodes with a given amplitude, frequency, and pulse width. Multiple cohorts are interleaved in a tonic fashion, targeting a specific area of the spinal cord to enhance excitability promoting supraspinal signals and sensory information integration. In most cases, individuals will have left and right differences requiring a left and right “swing phase” cohort. This cohort will be focused on either ankle dorsiflexion or hip flexion or a combination of both. Individuals having difficulty at any point of the swing phase might require multiple cohorts focused on this capacity. In addition, given the differences in electrode distribution and frequency required for standing, a single cohort or multiple cohorts focused on extension are required during the early phase of mapping.

Mapping is initially performed on the treadmill with body weight support. Initial speeds and body weight support are found without stimulation (Fig. 7d). The level of body weight support provided must maintain an upright posture during the gait cycle, while maximizing the load on the legs during the stance phase. Typical initial body weight support values range from 40% to 60% and are highly dependent on level of injury and available trunk control. Speeds assessed range from 0.36 m/s to 1.12 m/s. Both slow and fast speeds are used because a slow speed will allow better timing for integration of intent, whereas a fast speed will increase the excitability level of the spinal cord circuitry.³⁹ The excitability and coordination patterns observed without stimulation will also inform the team on the modulatory potential of spinal circuitry in the presence of appropriate sensory information. Once stimulation is turned on, the team first observes the integration of scES and sensory information and how motor output is modulated. If stimulation continues to allow integration to occur, and the motor output is appropriately modulated to the step cycle, flexors active during swing, and extensors during stance, the next step is to add intent (Fig. 6d). If stimulation generates an undesirable pattern, such as excessive flexion or excessive extension, that cannot be appropriately modulated with sensory information, the stimulation parameters must be changed.

Once intent is integrated into the mapping process, individuals will be asked to focus on a single component of the step cycle, that is, left leg flexion during swing. The team will observe how intent modulates the EMG for the specific side in addition to the contralateral side. If modulation occurs on the appropriate agonist muscles, but no independence is observed, the stimulation intensity can be increased on the desired cohort. Stimulation intensity can be increased until independence is achieved or stimulation becomes so strong that modulation is no longer appropriate. Care must be taken to ensure intent and/or an increase in stimulation does not cause the contralateral leg also to flex during the attempt.

Strategies that can be used in the optimization are slowing down the speed of the treadmill to allow individuals to have more time to coordinate the intent to phase of the step cycle and providing a general cohort, typically not side specific, that increases overall excitability of the network. This cohort becomes the key integrator for all additional cohorts and typically remains intact through future mapping adjustments. In most cases, a single leg will emerge as the “easier” leg, and that pattern will become automatic. A slow integration of other components and adjustment of configuration are typically required for coordinated stepping to emerge. The process of scES electrode configuration for stepping typically lasts two hours and can be performed in two to three days.

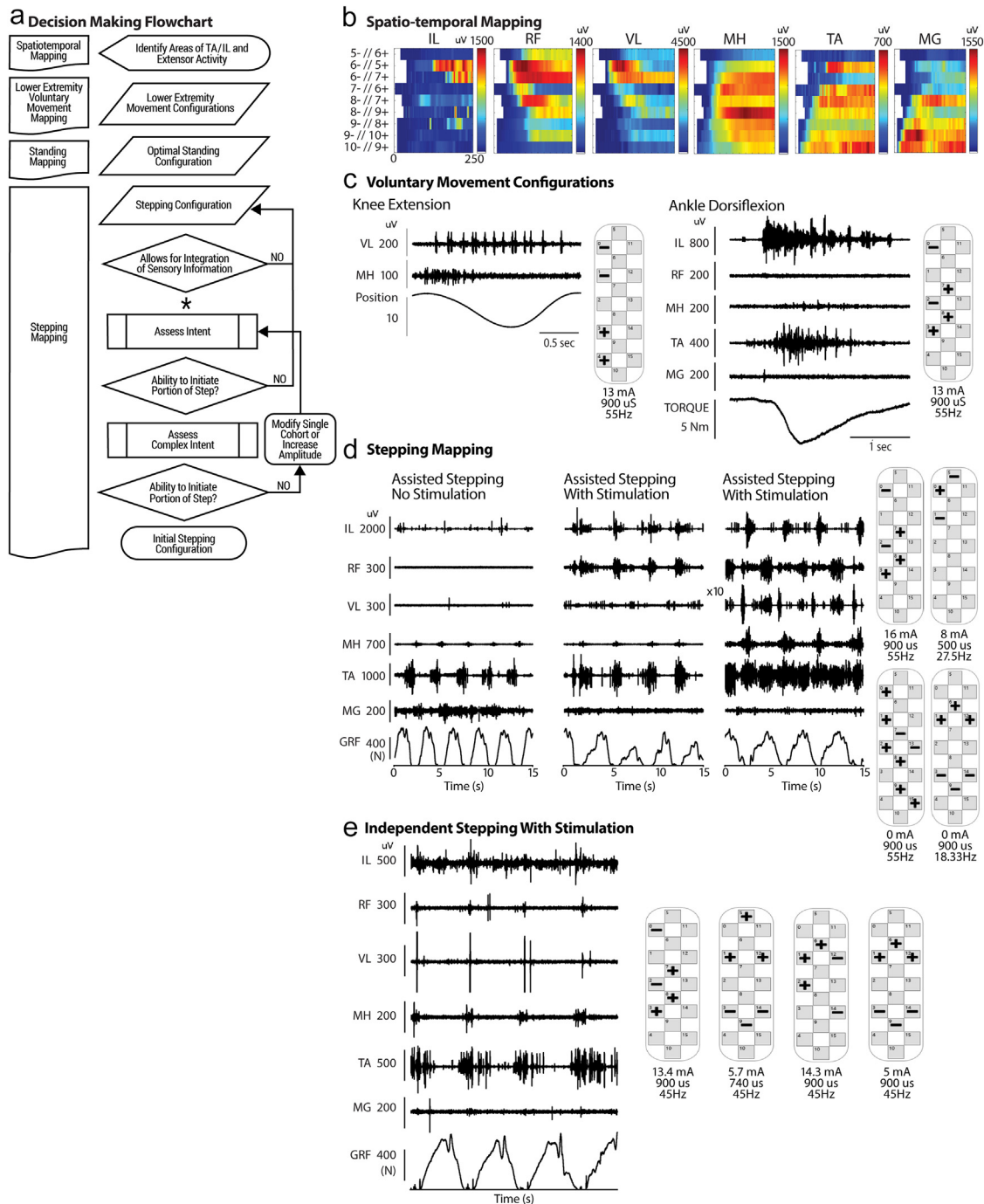


Figure 7. Selection of scES parameters for stepping. a. Decision-making chart for the selection of stepping configurations. Spatiotemporal mapping is used to identify the areas of the electrode array where TA and IL activity is present, in addition to extensor activity. Furthermore, the lower extremity voluntary mapping and standing mapping are used to examine optimal and suboptimal configuration. An initial configuration is represented as the data (parallelogram); decisions in the process are represented by rhomboids. If the response to the question is YES, one continues down the flowchart; if NO, the flowchart will guide one to the restarting point. A predefined process (rectangles) will expand on the assessments needed to optimize the configuration, and it is typically followed by a decision. An alternate process (rounded-corner rectangles) can be inserted late in the flow chart if a complex decision is not achieved, promoting a small modification to the configuration and restarting linking back to a predetermined process. The asterisk (*) signifies a stopping point if ability to initiate a step cannot be achieved during the mapping process. b. Color maps depicting the peak-to-peak amplitude values (μV) corresponding to stimulation current and electrode configuration (numbers in each row refer to contacts of the electrode array tested for the IL, RF, VL, MH, TA, and MG muscles). c. EMG activity of representative leg muscles during voluntary movement for knee extension and ankle dorsiflexion. The applied epidural stimulation programs are reported on the bottom left of the panel. d. EMG activity of representative leg muscles during stepping with no stimulation (left), with stimulation while assisted at different amplitudes. e. EMG activity of representative leg muscles during independent stepping. IL, iliopsoas; MG, medial gastrocnemius; TA, tibialis anterior.

Selection of scES Electrode Configuration for Cardiovascular Regulation

We perform all CV regulation mapping while the individual is sitting on their wheelchair. All research participants have weaned off any hypotensive drugs before study participation; similarly, abdominal binders are restricted during the mapping process. Caffeine consumption is not restricted before the mapping process. We first select the cathode distribution by identifying the location of L3–L4 spinal cord levels on the basis of the neuroanatomical 3D reconstruction model of spinal cord. The spatiotemporal mapping data identify those cathodes that may have modulated blood pressure without eliciting motor activity. The voluntary movement configuration provides information related to the frequencies and pulse widths optimized for motor activity. We select frequencies 20 to 30 Hz higher and pulse widths two to three times lower than those identified for motor activity. The objective of the higher frequencies is to prevent motor activation during stimulation for CV regulation. Frequency response data from spatiotemporal mapping will suggest that at approximately 60 Hz, the motor activation starts to decrease. Similarly, the lower pulse widths will generate lower leg activation at the same intensity. Both these strategies are used to minimize the potential for motor activity during CV regulation stimulation. We first select anodes directly adjacent to the selected cathodes and add more anodes if muscle activity occurs, selecting them on the basis of cathodes effective for motor activity (Fig. 8a). Next, we assess whether increasing amplitude directly increases systolic blood pressure, and if so, we increase the amplitude until the target range is reached (eg, 110–120 mm Hg systolic blood pressure). We selected a target range of 110 to 120 mm Hg systolic blood pressure during sitting; this range is within the healthy systolic blood pressure standards set by the American College of Cardiology.⁴⁰ When a targeted upper limit is reached or exceeded (eg, >120 mm Hg systolic blood pressure), we decrease the amplitude. We then assess for muscle activity adding anodes and/or increasing frequency if there are significant motor responses. More cohorts may be added to optimize the sensitivity of the blood pressure response and/or avoid muscle activity.

Selection of scES Electrode Configuration for Facilitating Bladder Storage and Emptying

Bladder mapping follows a human-guided interactive optimization approach⁴¹ in which the experimental mapping process is subdivided into separate domains/tasks to isolate parameters for storage function and the initiation of voiding (Fig. 9a). Because these domains are interdependent, subsequent optimization is used to test and refine parameters concurrently to build a comprehensive framework for multisystem stimulation.

Mapping sessions during filling cystometry for each participant are conducted in a sitting position and use cohorts (Fig. 9; CV) to stabilize blood pressure that is identified during CV mapping because bladder filling is a trigger for autonomic dysreflexia.⁴² We monitor the detrusor and urethral pressure responses and sphincter EMG responses during both storage and emptying phases (void attempts) to identify the bladder compliance (BC)-scES and bladder voiding (BV)-scES programs. The parameters (anode, cathode selection; frequency and amplitude, and number of cohorts) are adjusted to maintain stable blood pressure while achieving normative bladder capacity and BV. The goal for bladder capacity BC-scES is to reach fill volumes between 400 and 500 mL (based on average normal capacity and avoiding overdistention in

individuals performing intermittent catheterization four–six times per day [including average fluid intake]).^{43,44} The stimulation parameters are selected to reach the fill volume while also maintaining low filling detrusor pressures (<10 cmH₂O)^{45,46} to improve overall BC and detrusor leak-point pressures (<40 cmH₂O).⁴³ For void initiation (BV-scES), we target the sacral micturition center. The two programs (BC-scES and BV-scES) are used sequentially for the fill-void cycle.

On the basis of previously published methods,^{8,15} bladder mapping is performed by selecting electrode configurations with cathodes in three different locations. Cathodes positioned caudally target the sacral micturition center and parasympathetic pathways. Cathodes positioned in the midarray target the purported lumbar spinal coordinating center with presynaptic connections to sphincter motoneurons.^{47,48} Finally, cathodes positioned rostrally target sympathetic pathways (location selection order varied for each mapping session). Changes in detrusor pressure, sphincter activation/relaxation, and blood pressure responses are monitored while conducting a gradual ramp up of stimulation frequency and intensity until a near-motor threshold stimulation amplitude is selected that does not elicit direct lower limb movements. Stimulation frequency and intensity are then modulated synergistically to isolate an optimal frequency that elicits an overall continuous low detrusor-pressure filling profile with a synchronized sphincter EMG pattern effective for bladder continence. Guided by participants' sensations of bladder fullness, the transition from continence to micturition aims to integrate ascending inputs and descending volitional drive. Electrodes in the caudal, middle, and rostral regions of the array are selected while frequency is kept constant, and amplitude is adjusted to isolate an optimal intensity that drives the initiation of voiding activity (simultaneous increase in detrusor pressure with decrease in upper urethral pressure and quiescence of sphincter EMG responses). Electrode location and selection refinement is further modified to adjust for sensory and autonomic symptoms during mapping. Outcome data such as numbers of fillings per session (dependent on capacity), number of mapping sessions, and blood pressure monitoring can be found in our previously published articles.^{8,49,50}

Lower extremity and trunk EMG is monitored continuously throughout mapping to identify those parameters that modulate detrusor pressure and coordination with the external anal sphincter muscle (mirroring external urethral sphincter) but do not elicit motor activity in the lower extremity or trunk. Stimulation amplitude is lowered, frequency increased, and electrode selection modified to avoid lower extremity/trunk activity. All mapping urodynamic studies should be completed at least two days apart.

DISCUSSION

The motor and autonomic functional mapping methods for tonic-interleaved scES provide clear strategies for simultaneous recovery of the myriad of consequences of severe chronic SCI. Surgical placement is guided by anatomical markers obtained from the neuroanatomical 3D reconstruction model of the spinal cord, and intraoperative electrophysiology. In addition, we highlight the importance of spatiotemporal mapping before starting functional and physiological mapping. Spatiotemporal mapping provides a clear relationship between electrode location and motor activation. Owing to the high variability among injuries and neurophysiological profiles, mapping is a necessary strategy to personalize

stimulation configurations. Functional stimulation configurations are complex in nature, needing the integration of knowledge acquired during spatiotemporal mapping about stimulation thresholds, motor pool relationships, and frequency dependency. During functional mapping, small changes in electrode selection (polarity and location) can have various effects on motor activity and blood pressure regulation; understanding how these parameters affect relationships between agonistic and antagonistic muscles helps reduce the iterations needed to optimize stimulation.

Dimitrijevic et al presented early evidence of electrophysiological mapping in their work describing the capacity of the injured spinal cord to generate locomotor-like patterns in the presence of epidural stimulation.⁵¹ Minassian et al further presented evidence for electrophysiological dependency on cathode and anode position.^{35,52} Other groups have used spatiotemporal mapping as the initial strategy for the optimization of stimulation parameters.^{4,10,22,53} Although various strategies for stimulation and mapping have been used, ranging from those presented in this study to preference learning²³ and model-based personalized configuration libraries,¹² understanding electrophysiological and functional responses is key to identifying the initial

successful configurations for training. Some groups have used computational simulations and imaging technology to identify motor hot spots and recruitment relationships relative to dorsal root anatomy. These strategies are used to reduce the mapping iterations assessed in each individual.^{10,12,34} Similarly, computational simulations use electrode position relative to anatomical structures to derive potential stimulation outputs. For patterned spatial-temporal scES to be effective, it requires the delivery of recurring sequences of stimulation targeting specific motor hot spots at suprathreshold amplitudes. During training, wireless communication enables real-time control of stimulation parameters in which sequences of stimulation are pre-programmed in either open loop or triggered closed loop (by external sensors/signals).^{10,12,34} This strategy supersedes the afferent feedback and the autonomous interneuronal circuitry. In contrast, tonic-interleaved scES allows restoration of all essential functions of the spinal cord by receiving and integrating a variety of signals. Both strategies have been shown to be effective in restoring motor function in individuals with SCI.²¹

We have provided evidence that task-specific neuromodulation is governed by the stimulation parameters selected and ways activity-

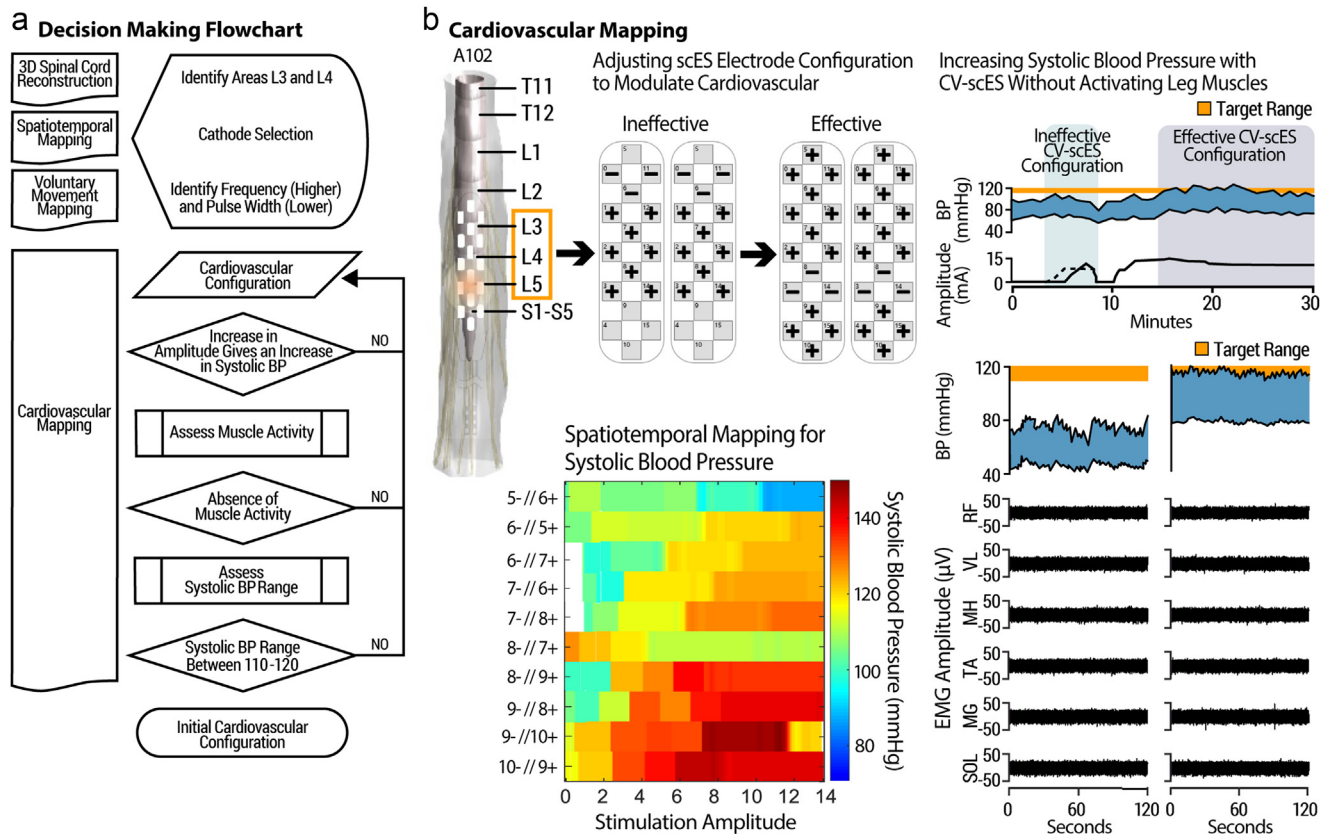


Figure 8. Selection of scES parameters for cardiovascular regulation. a. Decision-making flowchart for the selection of configurations for CV regulation. Spatiotemporal mapping for systolic blood pressure is used to identify the areas of the electrode array where blood pressure is modulated without EMG activity. In addition, the lower extremity voluntary mapping is used to examine the cathodes that promote movement. An initial configuration is represented as the data (parallelogram); decisions in the process are represented by rhomboids. If the response to the question is YES, one continues down the flowchart; if NO, the flowchart will guide one to the restarting point. A predefined process (rectangles) will expand on the assessments needed to optimize the configuration, and it is typically followed by a decision. An alternate process (rounded-corner rectangles) can be inserted late in the flow chart if a complex decision is not achieved, promoting a small modification to the configuration and restarting linking back to a predetermined process. b. Example of the flow of identifying the configuration, assessing the blood pressure response, and modifying the configuration to result in systolic blood pressure responding to normative levels. Color maps depicting the systolic blood pressure (mm Hg) corresponding to stimulation current and electrode configuration (numbers in each row refer to contacts of the electrode array tested used for identifying initial cathodes for blood pressure). Corresponding EMG activity of representative leg muscles with no activity when using CV-scES. BP, blood pressure; MG, medial gastrocnemius; TA, tibialis anterior.

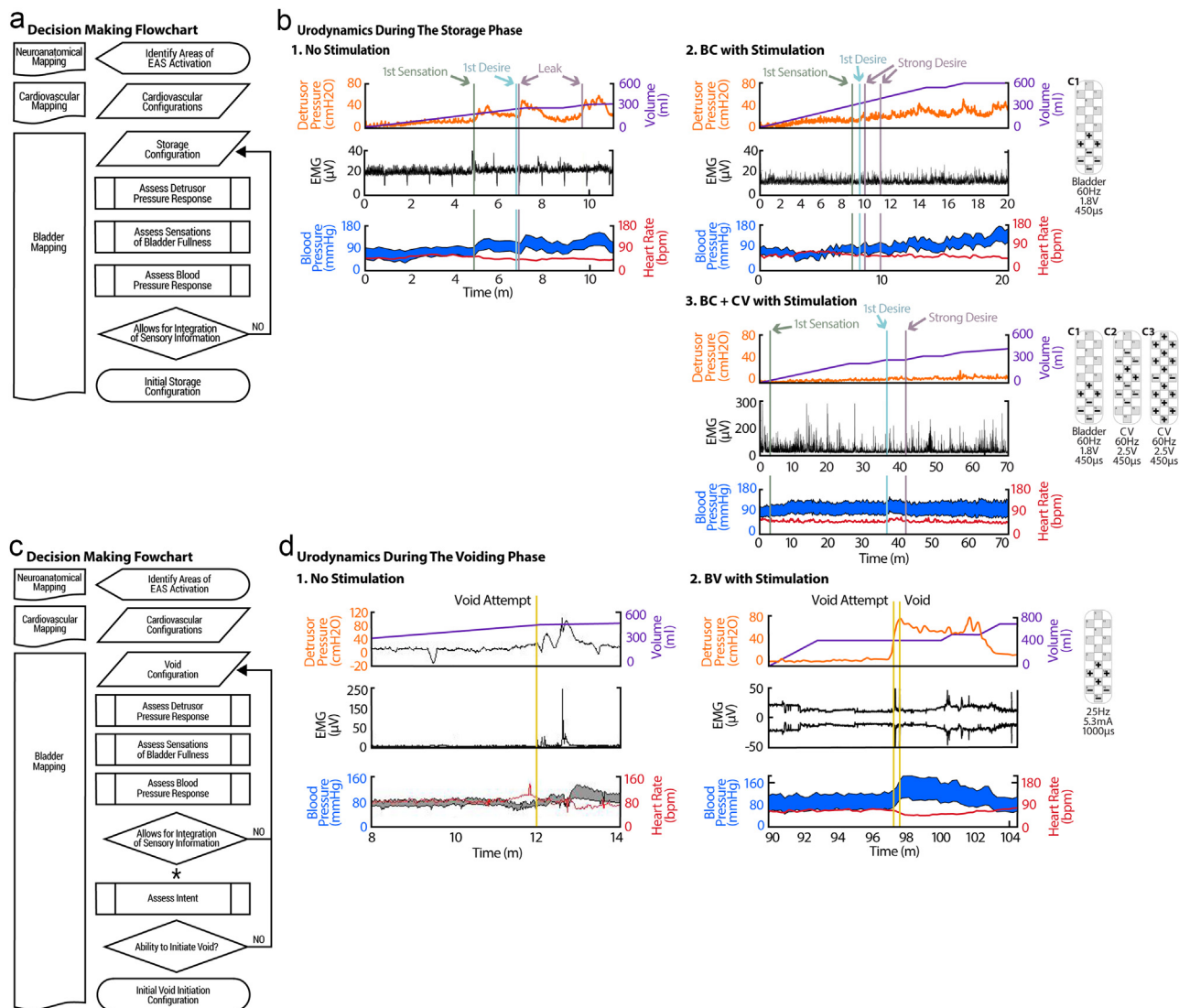


Figure 9. Selection of scES parameters for maintenance of bladder continence and the initiation of voiding. a. Decision-making flowchart for the selection of stimulation parameters for BC. Recording MRI axial scans with high spatial resolution (3 mm slice thickness and zero gap) were used to anatomically map the lumbosacral spinal cord region relative to the paddle array. Initial selection of scES parameters targeted the caudal region of the array, with activation of the striated sphincteric muscles of the perineum (EAS). Stimulation parameters targeting CV function were also integrated during bladder mapping to improve blood pressure stabilization at higher filling cystometry volumes. After the initial stimulation configuration (parallelogram) is defined, decisions in the process are represented by rectangles. If the response to the question is YES, the flow continues vertically down; if NO, the flowchart will guide one to a restarting point to allow small adjustments of the stimulation parameters, restarting back to a predetermined process. b1. Representative example of filling cystometry without stimulation. Note the rapid rise in detrusor pressure (red) during filling (volume in purple) and a concomitant elevation of blood pressure (blue), timed to each bladder contraction. Sensations of bladder fullness (vertical green and blue lines) coincide with detrusor overactivity and increased EMG activity (black) at low bladder capacity. Filling cystometry ceased owing to the loss of continence (light purple leaks) and systolic blood pressure elevation. Per our published urodynamic protocol in persons with SCI, bladder filling is ceased if one or more of the following conditions are observed: 1) spontaneous urine leakage, 2) infused volume >600 mL, 3) high intravesical pressure >40 cmH₂O, or 4) autonomic dysreflexia as evidenced by a sustained systolic blood pressure recording 20 mm Hg from baseline and/or intolerable symptoms.⁹ b2. Representative example of mapping for BC showing increased bladder capacity and reduced detrusor pressure. b3. Maintenance of both normal systolic blood pressure (target <120 mm Hg) and standard bladder filling pressure (<10 cmH₂O) during cystometry required both BC-scES and CV-scES cohorts (C1, and C2–C3, respectively). c. Decision-making flowchart for the selection of stimulation parameters for the initiation of BV. In case the mapping process does not result in the targeted functional outcome (initiation of voluntary voiding), stimulation configuration may be determined at the flowchart level identified with the asterisk (*). d1. Without using scES, the urologic profile during the voiding phase revealed detrusor contractions not sufficient to decompress the EAS activity during the void attempt. d2. Example of BV phase trace with stimulation showing a more synchronized detrusor-sphincter relationship, resulting in the generation of a bladder contraction from a stable filling pressure (<10 cmH₂O) sufficient to initiate voiding. Note that a uroflow was not tested in the mapping environment, and the EMG displayed reflects the linear envelope of the signal. A blood pressure response occurred beginning with the void attempt (start indicated with the first yellow vertical line), followed by a return to baseline values once voiding was initiated (indicated with the second yellow line), likely reflective of the participants' effort to empty. Cathode stimulating electrodes are represented with (–); anodes are represented with (+), and inactive electrodes are gray. Intensity is represented in volts (V for panel b) and milliamperes (mA) for panel d. Pulse width is in microseconds (µs); time in minutes (m). bpm, beats per minute; C, cohorts; cmH₂O, centimeters of water; EAS, external anal sphincter; Hz, frequency of the stimulation; mm Hg, millimeters of mercury; rEMG, electromyography in microvolts.

based recovery training integrates to result in motor recovery in those with chronic SCI.^{1–3} The state of the network excitability is a key parameter in executing motor tasks. By finding the relationship between electrode selection, frequency, and amplitude and the excitability state of the network, the researcher or clinician can control the modulation of the spinal circuitry and promote the integration of peripheral and supraspinal signals. Using a machine learning strategy, Mesbah et al developed a computational model that could classify with high accuracy (up to 97%) independent and assisted standing with scES, solely on the basis of EMG-frequency (by Continuous Wavelet Transform) and time-domain features.³⁸ This approach results in muscle-specific feedback on the effectiveness of scES-promoted muscle activation for standing. This tactic can be implemented to identify which of the tested sets of stimulation parameters promotes muscle activation more effectively for standing even if the same level of external assistance is required. In addition, it can contribute to detecting which muscle groups are not activated properly so that appropriate adjustments in stimulation parameters can be explored.

Integration of systems must be considered during the functional mapping process. Although not specifically detailed in this study, it is not hard to encounter an individual who requires blood pressure regulation during standing (Fig. 6e). In this case, knowledge of the optimized CV configuration will provide a starting point for integration with standing. Furthermore, understanding the components of the specific configurations that suppress muscle activity is critical in the integration process. Similarly, bladder storage configurations will most likely require a configuration to lower blood pressure. Multisystem integration for scES is achieved by interleaving configurations focused on two or more functions and is possible owing to the single optimized placement of the electrode array. Physiological control and regulation typically handled by various systems before injury can be integrated through optimized scES neuromodulation to allow patients with SCI to restore complex functions in the presence of stimulation.

Translation into clinical practice must follow some components of the approach to mapping presented in this study. The omission of spatiotemporal and functional mapping can lead to low levels of success and a potential disconnect between research outcomes and clinical outcomes. Although early optimization of configurations is thought to be time consuming and requiring electrophysiological knowledge, the associated benefit cannot be overstated. The institution of widely available data bases with successful configurations identified with associated information and training modules would accelerate the translation to use in the clinic. Introduction of artificial intelligence and learning algorithms can reduce the burden by optimizing the mapping procedures and proposing initial configurations. This will not only reduce the time needed for the mapping sessions but also potentially recommend functional configurations that provide an effective starting point for assessment.

Acknowledgements

The authors are indebted to the research participants for their courage, dedication, motivation, and perseverance that made these research findings possible. The authors thank Dr Jonathan Hodes for surgical procedures. Drs Glen Hirsch, Darryl Kaelin, Camilo Castillo, Marcus Stoddard, Todd Linsenmeyer, Kellen Choi, and Sarah Wagers provided medical oversight. Yukishia Austin, Lynn Robbins, and Kristen Johnson provided nursing medical

management. Yangsheng Chen and Sharon Zdunowski provided engineering leadership, and Taylor Blades and Christie Ferreira provided project management. Rebekah Morton, Justin Vogt, Katie Fields, Katelyn Brockman, Brittany Logsdon, Ricky Seither, Kristin Benton, Dylan Pfof, Eric Davis, and Aaron Bullock led research interventions and provided support to research participants.

Authorship Statements

Susan Harkema, Claudia Angeli, and Enrico Rejc designed and conducted the study, including patient recruitment. Claudia Angeli, Enrico Rejc, April Herrity, Samineh Mesbah, Charles Hubscher, and Susan Harkema conducted data collection, and data analysis with important intellectual input from Maxwell Boakye and Gail Forrest. Claudia Angeli, Enrico Rejc, Maxwell Boakye, April Herrity, Samineh Mesbah, Charles Hubscher, Gail Forrest, and Susan Harkema prepared the manuscript draft. All authors approved the final manuscript.

How to Cite This Article

Angeli C., Rejc E., Boakye M., Herrity A., Mesbah S., Hubscher C., Forrest G., Harkema S. 2023. Targeted Selection of Stimulation Parameters for Restoration of Motor and Autonomic Function in Individuals With Spinal Cord Injury. *Neuromodulation* 2023; ■: 1–16.

SUPPLEMENTARY DATA

To access the supplementary material accompanying this article, visit the online version of *Neuromodulation: Technology at the Neural Interface* at www.neuromodulationjournal.org and at <https://doi.org/10.1016/j.neurom.2023.03.014>.

REFERENCES

1. Angeli CA, Boakye M, Morton RA, et al. Recovery of over-ground walking after chronic motor complete spinal cord injury. *N Engl J Med*. 2018;379:1244–1250.
2. Rejc E, Angeli CA, Atkinson D, Harkema SJ. Motor recovery after activity-based training with spinal cord epidural stimulation in a chronic motor complete paraplegic. *Sci Rep*. 2017;7, 13476.
3. Rejc E, Angeli CA, Bryant N, Harkema SJ. Effects of stand and step training with epidural stimulation on motor function for standing in chronic complete paraplegics. *J Neurotrauma*. 2017;34:1787–1802.
4. Gill ML, Grahn PJ, Calvert JS, et al. Neuromodulation of lumbosacral spinal networks enables independent stepping after complete paraplegia. *Nat Med*. 2018;24:1677–1682.
5. Darrow D, Balsler D, Netoff TI, et al. Epidural spinal cord stimulation facilitates immediate restoration of dormant motor and autonomic supraspinal pathways after chronic neurologically complete spinal cord injury. *J Neurotrauma*. 2019;36:2325–2336.
6. Harkema SJ, Legg Ditterline B, Wang S, et al. Epidural spinal cord stimulation training and sustained recovery of cardiovascular function in individuals with chronic cervical spinal cord injury. *JAMA Neurol*. 2018;75:1569–1571.
7. Harkema SJ, Wang S, Angeli CA, et al. Normalization of blood pressure with spinal cord epidural stimulation after severe spinal cord injury. *Front Hum Neurosci*. 2018;12:83.
8. Herrity AN, Williams CS, Angeli CA, Harkema SJ, Hubscher CH. Lumbosacral spinal cord epidural stimulation improves voiding function after human spinal cord injury. *Sci Rep*. 2018;8:8688.
9. Hubscher CH, Herrity AN, Williams CS, et al. Improvements in bladder, bowel and sexual outcomes following task-specific locomotor training in human spinal cord injury. *PLoS One*. 2018;13:e0190998.
10. Wagner FB, Mignardot JB, Le Goff-Mignardot CG, et al. Targeted neurotechnology restores walking in humans with spinal cord injury. *Nature*. 2018;563:65–71.

11. Formento E, Minassian K, Wagner F, et al. Electrical spinal cord stimulation must preserve proprioception to enable locomotion in humans with spinal cord injury. *Nat Neurosci.* 2018;21:1728–1741.
12. Rowald A, Komi S, Demesmaeker R, et al. Activity-dependent spinal cord neuromodulation rapidly restores trunk and leg motor functions after complete paralysis. *Nat Med.* 2022;28:260–271.
13. Solinsky R, Specker-Sullivan L, Wexler A. Current barriers and ethical considerations for clinical implementation of epidural stimulation for functional improvement after spinal cord injury. *J Spinal Cord Med.* 2020;43:653–656.
14. Grahn PJ, Lavrov IA, Sayenko DG, et al. Enabling task-specific volitional motor functions via spinal cord neuromodulation in a human with paraplegia. *Mayo Clin Proc.* 2017;92:544–554.
15. Angeli CA, Edgerton VR, Gerasimenko YP, Harkema SJ. Altering spinal cord excitability enables voluntary movements after chronic complete paralysis in humans. *Brain.* 2014;137:1394–1409.
16. Harkema S, Gerasimenko Y, Hodes J, et al. Effect of epidural stimulation of the lumbosacral spinal cord on voluntary movement, standing, and assisted stepping after motor complete paraplegia: a case study. *Lancet.* 2011;377:1938–1947.
17. Mesbah S, Ball T, Angeli C, et al. Predictors of volitional motor recovery with epidural stimulation in individuals with chronic spinal cord injury. *Brain.* 2021;144:420–433.
18. Rejc E, Angeli C, Harkema S. Effects of lumbosacral spinal cord epidural stimulation for standing after chronic complete paralysis in humans. *PLOS ONE.* 2015;10:e0133998.
19. Rejc E, Smith AC, Weber 2nd KA, et al. Spinal cord imaging markers and recovery of volitional leg movement with spinal cord epidural stimulation in individuals with clinically motor complete spinal cord injury. *Front Syst Neurosci.* 2020;14:559313.
20. Squair JW, Gautier M, Mahe L, et al. Neuroprosthetic baroreflex controls haemodynamics after spinal cord injury. *Nature.* 2021;590:308–314.
21. Harkema S, Angeli C, Gerasimenko Y. Historical development and contemporary use of neuromodulation in human spinal cord injury. *Curr Opin Neurol.* 2022;35:536–543.
22. Hoglund BK, Zurn CA, Madden LR, et al. Mapping spinal cord stimulation-evoked muscle responses in patients with chronic spinal cord injury. *Neuromodulation.* Published online December 12, 2022. <https://doi.org/10.1016/j.neurom.2022.10.058>
23. Zhao Z, Ahmadi A, Hoover C, et al. Optimization of spinal cord stimulation using Bayesian preference learning and its validation. *IEEE Trans Neural Syst Rehabil Eng.* 2021;29:1987–1997.
24. Hofstoetter US, Perret I, Bayart A, et al. Spinal motor mapping by epidural stimulation of lumbosacral posterior roots in humans. *iScience.* 2021;24:101930.
25. Capogrosso M, Wagner FB, Gandar J, et al. Configuration of electrical spinal cord stimulation through real-time processing of gait kinematics. *Nat Protoc.* 2018;13:2031–2061.
26. Preeti MC. MRI study of level of termination of spinal cord (Conus medullaris). *Int J Sci Res.* 2016;5:122–124.
27. Mesbah S, Herrity A, Ugiliweneza B, et al. Neuroanatomical mapping of the lumbosacral spinal cord in individuals with chronic spinal cord injury. *Brain Commun.* 2022;5:fcac330.
28. Toossi A, Bergin B, Marefatallah M, et al. Comparative neuroanatomy of the lumbosacral spinal cord of the rat, cat, pig, monkey, and human. *Sci Rep.* 2021;11:1955.
29. Toossi A, Everaert DG, Perlmutter SI, Mushahwar VK. Functional organization of motor networks in the lumbosacral spinal cord of non-human primates. *Sci Rep.* 2019;9:13539.
30. Geiringer SR. *Anatomic Localization for Needle Electromyography.* Hanley & Belfus; 1999.
31. Mesbah S, Angeli CA, Keynton RS, El-Baz A, Harkema SJ. A novel approach for automatic visualization and activation detection of evoked potentials induced by epidural spinal cord stimulation in individuals with spinal cord injury. *PLoS One.* 2017;12:e0185582.
32. Jilge B, Minassian K, Rattay F, et al. Initiating extension of the lower limbs in subjects with complete spinal cord injury by epidural lumbar cord stimulation. *Exp Brain Res.* 2004;154:308–326.
33. Sayenko DG, Angeli C, Harkema SJ, Edgerton VR, Gerasimenko YP. Neuro-modulation of evoked muscle potentials induced by epidural spinal-cord stimulation in paralyzed individuals. *J Neurophysiol.* 2014;111:1088–1099.
34. Capogrosso M, Wenger N, Raspopovic S, et al. A computational model for epidural electrical stimulation of spinal sensorimotor circuits. *J Neurosci.* 2013;33:19326–19340.
35. Minassian K, Jilge B, Rattay F, et al. Stepping-like movements in humans with complete spinal cord injury induced by epidural stimulation of the lumbar cord: electromyographic study of compound muscle action potentials. *Spinal Cord.* 2004;42:401–416.
36. Murg M, Binder H, Dimitrijevic MR. Epidural electric stimulation of posterior structures of the human lumbar spinal cord: 1. Muscle twitches – a functional method to define the site of stimulation. *Spinal Cord.* 2000;38:394–402.
37. Rattay F, Minassian K, Dimitrijevic MR. Epidural electrical stimulation of posterior structures of the human lumbosacral cord: 2. Quantitative analysis by computer modeling. *Spinal Cord.* 2000;38:473–489.
38. Mesbah S, Gonnelli F, Angeli CA, El-Baz A, Harkema SJ, Rejc E. Neurophysiological markers predicting recovery of standing in humans with chronic motor complete spinal cord injury. *Sci Rep.* 2019;9:14474.
39. Beres-Jones JA, Harkema SJ. The human spinal cord interprets velocity-dependent afferent input during stepping. *Brain.* 2004;127:2232–2246.
40. Whelton PK, Carey RM, Aronow WS, et al. 2017 ACC/AHA/AAPA/ABC/ACPM/AGS/APHA/ASH/ASPC/NMA/PCNA guideline for the prevention, detection, evaluation, and management of high blood pressure in adults: a report of the American College of Cardiology/American Heart Association Task Force on clinical practice guidelines. *Hypertension.* 2018;71:e13–e115.
41. Klau GW, Lesh N, Marks J, Mitzenmacher M. Human-guided search. *J Heuristics.* 2010;16:289–310.
42. Faaborg PM, Christensen P, Krassioukov A, Laurberg S, Frandsen E, Krogh K. Autonomic dysreflexia during bowel evacuation procedures and bladder filling in subjects with spinal cord injury. *Spinal Cord.* 2014;52:494–498.
43. Rosier PF. The evidence for urodynamic investigation of patients with symptoms of urinary incontinence. *F1000Prime Rep.* 2013;5:8.
44. Consortium for Spinal Cord Medicine. Bladder management for adults with spinal cord injury: a clinical practice guideline for health-care providers. *J Spinal Cord Med.* 2006;29:527–573.
45. Schäfer W, Abrams P, Liao L, et al. Good urodynamic practices: uroflowmetry, filling cystometry, and pressure-flow studies. *NeuroUrol Urodyn.* 2002;21:261–274.
46. Abrams P, Cardozo L, Fall M, et al. The standardisation of terminology of lower urinary tract function: report from the Standardisation Sub-Committee of the International Continence Society. *NeuroUrol Urodyn.* 2002;21:167–178.
47. Chang HY, Cheng CL, Chen J-J, de Groat WCd. Serotonergic drugs and spinal cord transections indicate that different spinal circuits are involved in external urethral sphincter activity in rats. *Am J Physiol Renal Physiol.* 2007;292:F1044–F1053.
48. Karnup SV, de Groat WC. Propriospinal neurons of L3-L4 segments involved in control of the rat external urethral sphincter. *Neuroscience.* 2020;425:12–28.
49. Herrity AN, Hubscher CH, Angeli CA, Boakye M, Harkema SJ. Impact of long-term epidural electrical stimulation enabled task-specific training on secondary conditions of chronic paraplegia in two humans. *J Spinal Cord Med.* 2021;44:513–514.
50. Herrity AN, Aslan SC, Mesbah S, et al. Targeting bladder function with network-specific epidural stimulation after chronic spinal cord injury. *Sci Rep.* 2022;12:11179.
51. Dimitrijevic MR, Gerasimenko Y, Pinter MM. Evidence for a spinal central pattern generator in humans. *Ann N Y Acad Sci.* 1998;860:360–376.
52. Minassian K, Persy I, Rattay F, Pinter MM, Kern H, Dimitrijevic MR. Human lumbar cord circuitries can be activated by extrinsic tonic input to generate locomotor-like activity. *Hum Mov Sci.* 2007;26:275–295.
53. Calvert JS, Grahn PJ, Strommen JA, et al. Electrophysiological guidance of epidural electrode array implantation over the human lumbosacral spinal cord to enable motor function after chronic paralysis. *J Neurotrauma.* 2019;36:1451–1460.